2019

# Analytical investigation on the behavior of circular and square RC columns strengthened with RPC and wrapped with FRP under uniaxial compression

Atheer Hilal Mahdi Al - Gburi
*University of Wollongong*, ahmag930@uowmail.edu.au

M Neaz Sheikh
*University of Wollongong*, msheikh@uow.edu.au

Muhammad N. S Hadi
*University of Wollongong*, mhadi@uow.edu.au

## Abstract

This paper presents an analytical approach to predict the uniaxial compression behavior of circular and square reinforced concrete (RC) columns strengthened with reactive powder concrete (RPC) jackets and wrapped with fiber reinforced polymer (FRP). The analytical axial load-axial strain responses of the strengthened RC columns were compared with experimental axial load-axial strain responses. The analytical approach presented in this study conservatively predicted the ultimate axial load of the strengthened RC columns. Also, a parametric study was carried out to investigate key factors that influence the axial load-axial strain response of the strengthened RC columns. It was found that the ratio of the RPC jacket thickness to the diameter or side length of the base RC column significantly influenced the service axial load, ultimate axial load and ductility of a strengthened RC column.

# Analytical Investigation on the Behavior of Circular and Square RC Columns Strengthened with RPC and Wrapped with FRP under Uniaxial Compression

Atheer H.M. Algburi [1], M. Neaz Sheikh [2] and Muhammad N.S. Hadi [3*]

[1]Ph.D. Candidate, School of Civil, Mining and Environmental Engineering, University of Wollongong, NSW 2522, Australia. E-mail address: ahmag930@uowmail.edu.au.

[2]Associate Professor, School of Civil, Mining and Environmental Engineering, University of Wollongong, NSW 2522, Australia. E-mail address: msheikh@uow.edu.au.

[3*]Associate Professor, School of Civil, Mining and Environmental Engineering, University of Wollongong, NSW 2522, Australia, [*]Corresponding Author, E-mail address: mhadi@uow.edu.au, Tel.: +61 2 4221 4762; Fax: +61 2 4221 3238.

**Abstract**

This paper presents an analytical approach to predict the uniaxial compression behavior of circular and square reinforced concrete (RC) columns strengthened with reactive powder concrete (RPC) jackets and wrapped with fiber reinforced polymer (FRP). The analytical axial load-axial strain responses of the strengthened RC columns were compared with experimental axial load-axial strain responses. The analytical approach presented in this study conservatively predicted the ultimate axial load of the strengthened RC columns. Also, a parametric study was carried out to investigate key factors that influence the axial load-axial strain response of the strengthened RC columns. It was found that the ratio of the RPC jacket thickness to the diameter or side length of the base RC column significantly influenced the service axial load, ultimate axial load and ductility of a strengthened RC column.

Keywords:
Reinforced concrete; Columns; Jacketing; Reactive powder concrete; Analytical investigation.

## 1. Introduction

Reinforced concrete (RC) columns in vital infrastructure such as high-rise buildings and highway bridges may need to be rehabilitated due to a number of reasons. These reasons include deterioration due to the corrosion of steel reinforcement, inadequate design, functional changes and construction errors. Jacketing with RC is one of the most widely practiced techniques for strengthening deficient RC columns because of the ease of the construction and availability of the construction materials [1-3]. The traditional RC jacket is usually applied to the RC column by casting a concrete layer reinforced with steel bars and ties or with welded wire fabric around the column. The strength, stiffness and ductility of the deficient RC columns improve by the RC jacket [4, 5]. However, jacketing with RC is associated with a few disadvantages including increases in the dead load, requirements for the dowelling and anchoring with the base RC column, slow progress of the construction and decrease in the available space of the strengthened structure [1, 3].

Several studies investigated the behavior of RC columns strengthened with high strength RC jackets. Takeuti et al. [6] revealed that the use of high strength RC jacket decreased the thickness of the jacket and achieved the required load capacity. However, the concentrically loaded RC column strengthened with high strength RC jacket usually shows a quasi-linear response up to the maximum axial load followed by a sudden drop in the axial load [7]. Jacketing with high strength RC also has disadvantages similar to the jacketing with normal strength RC including the dowelling and anchoring with base RC columns.

Jacketing with steel has been widely used for retrofitting RC columns. However, steel jackets experience poor corrosion resistance. Steel jackets may also experience buckling during the installation and service life [8, 9].

Structural rehabilitation of RC columns with fiber reinforced polymer (FRP) has been increased rapidly worldwide. The FRP composite has a high strength to weight ratio and high corrosion resistance. From a practical point of view, the FRP composite can be easily wrapped around RC columns [9, 10]. It is well known that the strengthening of RC columns with FRP depends mainly on the lateral confinement pressure [8]. However, the confinement pressure decreases when RC columns are subjected to eccentric axial loads [11, 12, 13, 14]. Also, confinement pressure decreases with the increase in the diameter of the column. Moreover, FRP wrapping provides only a negligible enhancement in the yield strength and maximum flexural load of RC columns [15]. Although circular FRP jackets generate uniform confinement pressures onto the concrete column, square FRP jackets generate nonuniform confinement pressures onto the concrete column due to the stresses concentration at the corners of the column. As a result, the confinement efficiency of square FRP jackets is less than the confinement efficiency of circular FRP jackets [16].

The shape modification of the square columns to circular columns is one of the techniques used for improving the confinement efficiency of square RC columns [13]. Precast segments constructed with normal and high strength concrete were used as shape modifiers for square RC columns [13, 17]. However, it was found that precast concrete segments can be damaged during the installation with the concrete core [17]. Therefore, precast segments constructed with steel fiber reinforced concrete were recommended [17].

The reactive powder concrete (RPC) is a high-performance concrete with a dense structure containing fine particles graded to compact efficiently [18, 19]. The homogeneous structure and the presence of steel fiber within the matrix decreases the differential tensile strain and increases the energy absorption of the RPC [19]. Lee et al. [20] and Chang et al. [21] used the RPC as a novel repairing and strengthening material for small concrete specimens. Hadi et al. [22] and Algburi et al. [23] used the RPC jacket and FRP wrapping as a new jacketing system for strengthening RC columns. In Hadi et al. [22], circular RC column specimens were strengthened by a thin layer of RPC and wrapped with carbon fiber reinforced polymer (CFRP). The specimens were tested under concentric axial load, eccentric axial loads and four-point bending. It was found that jacketing with RPC and wrapping with FRP was an effective technique for increasing the yield load, ultimate load and energy absorption of circular deficient RC columns.

Algburi et al. [23] used the RPC as a new shape modification and strengthening material for square RC columns. The square RC column specimens were circularized with RPC jackets, wrapped with CFRP and tested under concentric axial load, eccentric axial loads and four-point bending. The RPC was found to be an efficient shape modification material for the square RC columns. Circularization of the square RC column specimens with the RPC jackets increased the yield load, ultimate load and energy absorption of the specimens significantly. It was also found that wrapping the RPC strengthened columns with FRP increased the ultimate load and energy absorption of the columns.

It is evident that the jacketing systems proposed in Hadi et al. [22] and Algburi et al. [23] were effective for strengthening the circular and square RC columns, respectively. However, a significant number of experimental and theoretical studies are required before the wide practical application of these jacketing systems. Hence, the aim of this paper is to develop an analytical approach for the axial load-axial strain responses of circular and square RC columns strengthened with RPC jackets and wrapped with FRP.

This paper presents an analytical approach for investigating the responses of the circular and square RC columns strengthened with RPC jackets and wrapped with FRP under axial compression. This paper also presents a parametric study to investigate the most important parameters that influence the axial load-axial strain responses of the strengthened circular and square RC columns. The parametric study investigates the influence of confinement ratio, unconfined compressive strength of the RPC jacket and the ratio of the RPC jacket thickness to the diameter or side length of the base RC column on the axial load-axial strain response, ductility and service axial load of the strengthened RC column. The analytical approach developed in this study can be used as a guideline for strengthening deficient RC columns.

## 2. Development of the analytical axial load-axial strain responses of the strengthened RC columns

### *2.1. Theoretical assumptions*

In this study, a deficient circular RC column with a diameter $d$ and area of longitudinal steel bars $A_s$ is assumed to be strengthened with a circular RPC jacket and wrapped with FRP. The RPC jacket is assumed to have a constant thickness $t$. Also, a deficient square RC column with a side length $b$ is assumed to be circularized with RPC jacket and wrapped with FRP. The RPC jacket for the square RC column is assumed to have a thickness $t_1$ at the middle of the square section and a thickness $t_2$ at the corners of the square section. The strengthened circular and square RC columns are assumed to have a diameter $D$. Figure 1 shows the cross-sections of circular and square RC columns constructed with normal strength concrete (NSC), strengthened with RPC and wrapped with FRP.

The axial load of circular or square RC column strengthened with RPC jacket and FRP wrapping is assumed to be the summation of the axial load components of the confined NSC of the core, confined RPC of the jacket, and longitudinal steel bars. The experimental axial load-axial strain responses of the specimens tested by Hadi et al. [22] and Algburi et al. [23] showed that confinement of the RPC jacket and the internal lateral steel reinforcement did not influence the axial load-axial strain response of the specimens up to the ultimate axial load. However, the confinement effect of the lateral steel reinforcement was significant after the ultimate axial load and the columns achieved a softening response. The softening response represents the behavior of the base RC column. As this study investigates analytically the responses of the strengthened RC columns up to the ultimate axial load, the confinement effect of the lateral steel reinforcement was ignored.

Figure 2 shows the conferment effect of the FRP on the RPC jacket and the concrete core of the base RC column. It is noted that both NSC and RPC in the strengthened columns are subjected to the same external lateral confinement pressure by the FRP wrapping. Therefore, the axial load of the strengthened RC columns calculated in this study took into the account the axial compressive stress of the FRP-confined NSC for the core, the axial compressive stress of the FRP-confined RPC of the jacket and the axial compressive stress of the longitudinal steel bars.

*2.2. Modelling of NSC, RPC and longitudinal steel bars*

In this study, a full bond between the deformed steel bars and the NSC core as well as a full bond between the RPC jacket and the NSC core were assumed to be achieved. The last assumption was based on the studies of Hadi et al. [22] and Algburi et al. [23] in which a full bond between the RPC jacket and the NSC core was achieved by adequately preparing the surface of the base RC column. Therefore, the axial compressive strains in the NSC, RPC and the longitudinal steel bars were assumed to be equal up to the ultimate axial load.

Over the last two decades, several models were presented to depict the response of the FRP-confined concrete under uniaxial compressive load [9, 24, 25]. The model proposed by Lam and Teng [25] for the FRP-confined concrete in circular columns was adopted in both ACI 440.2R-2008 [26] and ACI 440.2R-2017 [27]. Also, Lam and Teng [25] model was validated with a large experimental testing database. Therefore, the FRP-confined compressive stress of the NSC ($f_{cco}$) for a given axial compressive strain of $\varepsilon_c$ was calculated using the stress-strain model in ACI 440.2R-2017 [27], as follows:

$$f_{cco} = \begin{cases} E_{co}\varepsilon_c - \dfrac{(E_{co} - E_{2o})^2}{4f'_{co}}{\varepsilon_c}^2 & 0 \leq \varepsilon_c \leq \varepsilon_{to} \\ f'_{co} + E_{2o}\varepsilon_c & \varepsilon_{to} \leq \varepsilon_c \leq \varepsilon_{cco} \end{cases} \tag{1}$$

$$\varepsilon_{to} = \frac{2f'_{co}}{E_{co} - E_{2o}} \tag{2}$$

$$E_{2o} = \frac{f'_{ccof} - f'_{co}}{\varepsilon_{cco}} \tag{3}$$

$$E_{co} = 4730\sqrt{f'_{co}} \tag{4}$$

where $f'_{co}$ is the unconfined compressive strength of the NSC. The $f'_{cco}$ is the FRP-confined compressive strength of the NSC.

The $f'_{cco}$ was calculated using Eq. (5) [27].

$$f'_{cco} = f'_{co} + 3.3\Psi_f k_a f_l \tag{5}$$

where $\Psi_f$ is a reduction factor, which was taken as 0.95 [27] and $k_a$ is a shape modification factor, which was taken as 1 [27].

The $f_l$ is the lateral confinement pressure by the FRP, which was calculated using Eq. (6).

$$f_l = \frac{2nt_f E_f \varepsilon_{fe}}{D} \tag{6}$$

where $n$ is the number of the FRP layers, $t_f$ is the thickness of the FRP layer, $E_f$ is the modulus of elasticity of the FRP layer and $\varepsilon_{fe}$ is the effective strain of the FRP layer.

In ACI 440.2R-2017 [27], $\varepsilon_{fe}$ is recommended to be $0.55\varepsilon_{fu}$, where $\varepsilon_{fu}$ is the ultimate tensile strain of the FRP determined by the flat coupon test.

The $\varepsilon_{cco}$ is the compressive strain of the NSC corresponding to the FRP-confined compressive strength of the NSC. The $\varepsilon_{cco}$ was calculated using Eq. (7) [27].

$$\varepsilon_{cco} = \varepsilon_{co}\left[1.5 + 12k_b \frac{f_l}{f'_{co}}\left(\frac{\varepsilon_{fe}}{\varepsilon_{co}}\right)^{0.45}\right] \leq 0.01 \tag{7}$$

In Eq. (7), $\varepsilon_{co}$ is the compressive strain of the unconfined NSC at $f'_{co}$, kb is the shape modification factor, which was taken as 1 [27].

It is important to note that ACI 440.2R-2017 [27] reported that improvement in strength of concrete having compressive strength equals to or more than 70 MPa should be based on experimental results. Several experimental studies showed that the axial strength of RPC columns with compressive strengths of 110-160 MPa was improved by FRP wrapping [19, 22, 23]. Xiao et al. [28] revealed that the models proposed for the confined compressive strength of the NSC closely predicted the confined compressive strength of the high strength concrete. Therefore, the FRP-confined compressive stress of the RPC jacket ($f_{ccj}$) was modelled using the stress-strain model in ACI 440.2R-2017 [27] as:

$$f_{ccj} = \begin{cases} E_{cj}\varepsilon_c - \dfrac{\left(E_{cj} - E_{2j}\right)^2}{4f'_{cj}}\varepsilon_c{}^2 & 0 \leq \varepsilon_c \leq \varepsilon_{tj} \\ f'_{cj} + E_{2j}\varepsilon_c & \varepsilon_{tj} \leq \varepsilon_c \leq \varepsilon_{ccj} \end{cases} \tag{8}$$

$$\varepsilon_{tj} = \frac{2f'_{cj}}{E_{cj} - E_{2j}} \tag{9}$$

$$E_{2j} = \frac{f'_{ccj} - f'_{cj}}{\varepsilon_{ccj}} \tag{10}$$

where $f'_{cj}$ is the unconfined compressive strength of the RPC and $E_{cj}$ is the modulus of elasticity of the RPC. The $E_{cj}$ was calculated using Eq. (11), which was proposed by Ahmad et al. [29].

$$E_{cj} = 4360\sqrt{f'_{cj}} \quad (11)$$

The $f'_{ccj}$ is the FRP-confined compressive strength of the RPC, which was calculated using Eq. (12) [27].

$$f'_{ccj} = f'_{cj} + 3.3\Psi_f k_a f_l \quad (12)$$

The $\varepsilon_{ccj}$ is the compressive strain of the RPC jacket corresponding to the confined compressive strength of the RPC, which was calculated using Eq. (13) [27].

$$\varepsilon_{ccj} = \varepsilon_{cj}\left[1.5 + 12k_b \frac{f_l}{f'_{cj}}\left(\frac{\varepsilon_{fe}}{\varepsilon_{cj}}\right)^{0.45}\right] \leq 0.01 \quad (13)$$

where $\varepsilon_{cj}$ is the axial compressive strain of the unconfined RPC at $f'_{cj}$.

To model the axial compressive stress in the longitudinal steel bars ($f_s$), an elastic–perfectly plastic model was used.

$$f_s = E_s\varepsilon_c \leq f_y \quad (14)$$

where $E_s$ is the modulus of elasticity of steel, which can be taken as 200 GPa and $f_y$ is the yield strength of steel.

The axial load of circular and square RC columns strengthened with RPC jacket and FRP wrapping was calculated using Eq. (15).

$$N_t = f_{ccj}(A_t - A_g) + f_{cco}(A_g - A_s) + A_s f_s \qquad 0 \le \varepsilon_c \le \varepsilon_{ccj} \qquad (15)$$

where $N_t$ is the axial load of the strengthened RC column, $A_t$ is the total cross-sectional area of the strengthened RC column and $A_g$ is the gross cross-sectional area of the base RC column.

It is noted that the experimental axial load-axial strain responses for the strengthened circular and square RC columns showed three ascending branches. The first branch represents the response of unconfined NSC core and unconfined RPC jacket, the second branch represents the response of confined NSC core and unconfined RPC jacket and the third branch represents the response of confined NSC core and confined RPC jacket. However, all the available stress-strain models were derived to illustrate the response for concrete columns having one type of concrete. These models usually present the response of concrete column in two branches represent the unconfined concrete and confined concrete, respectively. For NSC, the confinement effect usually occurs at an axial compressive strain of about 0.002, which represents the compressive axial strain corresponding to $f'_{co}$. Therefore, the analytical axial load-axial strain in this study is presented in two branches. The first branch is up to an axial strain of 0.002 and the second branch is up to $\varepsilon_{ccj}$.

The axial loads calculated using Eq. (15) were generally higher than the experimental axial loads for the axial strains higher than 0.002. This was probably because of the multiple confinement effect of the NSC and RPC in the second branch of the axial load-axial strain response (after compressive strain of 0.002). In the second branch, the RPC was not confined up to an axial compressive strain of about 0.003. After the axial compressive strain of 0.003, the confinement effect of RPC started. However, the confinement efficiency of the RPC is less than that of the NSC. The different confinement efficiencies of the NSC and RPC may complicate the calculations and lead to a non-conservative ultimate analytical axial load. Therefore, reduction factors were used for the compressive stresses of the NSC and RPC corresponding to the axial compressive strains higher than 0.002. As a result, the final axial load of circular and square RC column strengthened with RPC jacket and FRP wrapping at any axial compressive strain were calculated as follows:

$$N_t = f_{ccj}(A_t - A_g) + f_{cco}(A_g - A_s) + A_s f_s \qquad 0 \leq \varepsilon_c \leq 0.002 \qquad (16.1)$$

$$N_t = 0.72 f_{ccj}(A_t - A_g) + 0.85 f_{cco}(A_g - A_s) + A_s f_s \qquad 0.002 < \varepsilon_c \leq \varepsilon_{ccj} \qquad (16.2)$$

where 0.72 and 0.85 are reduction factors. The reduction factors have been included to achieve a conservative ultimate analytical axial loads. Also, the column behavior changed from a quasi-bilinear behavior to an initial quasi-linear behavior followed by a transition region with softening response then linear ascending response. The last behavior agrees with the observed behavior of FRP-confined ultra-high strength concrete investigated in a recent study by de Oliveira et al. [30]. Since the RPC is considered an ultra-high strength concrete, the use of the reduction factors was required to match the behavior of the FRP-confined RPC in axial load-axial strain response of strengthened RC column. Eqs. (16.1) and (16.2) are proposed to depict the axial load-axial strain response of base RC column constructed from NSC of compressive strength 20 MPa to 50 MPa and strengthened with RPC of compressive strength ≥ 95 MPa then wrapped with FRP.

*2.3 Service axial load of the strengthened RC columns*

Under the service axial load, the concrete of the base RC column and the strengthened RC column should not reach the lateral cracking strain. Also, the longitudinal steel bars should not reach the yield strain [15]. Therefore, ACI 440.2R-17 [27] limits the service stress in the concrete to 60% of the compressive strength of concrete and the service stress in the steel to 80% of the yield strength of steel. In this study, the service axial load of the circular or square RC column strengthened with RPC and wrapped with FRP ($S_l$) was calculated from the transformed-section analysis using Eqs. (17), (18) and (19) whichever is lower.

$$S_l = \frac{0.6f'_{cco}}{E_c}\left[E_j\left(A_t - A_g\right) + E_c\left(A_g - A_s\right) + E_s A_s\right] \quad (17)$$

$$S_l = \frac{0.8f_y}{E_s}\left[E_j\left(A_t - A_g\right) + E_c\left(A_g - A_s\right) + E_s A_s\right] \quad (18)$$

$$S_l = \frac{0.6f'_{ccj}}{E_j}\left[E_j\left(A_t - A_g\right) + E_c\left(A_g - A_s\right) + E_s A_s\right] \quad (19)$$

*2.4 Ductility of the strengthened RC columns*

The ductility of the strengthened RC columns in this study was calculated based on energy absorption. The ductility was calculated as the area under the axial load-axial strain curve up to the axial compressive strain corresponding to the ultimate axial load to the area under the axial load-axial strain curve up to the axial compressive strain of 0.002. The axial compressive strain of 0.002 was assumed to represent the yield axial strain. This is because the axial compressive strain of 0.002 corresponds to the unconfined compressive strength of NSC core and is lower than the yield strain of steel bars [31].

## 3. Experimental program and results

### *3.1. Description of the specimens*

This section presents the experimental results of base and strengthened RC column specimens tested under concentric axial load. Full details about the preparation of the specimens and testing procedure can be found in Hadi et al. [22] and Algburi et al. [23]. Each of these two studies involved testing 16 column specimens, and in this study only two specimens are considered from each of these studies. In Hadi et al. [22], two circular RC column specimens were constructed from NSC. One of these two circular RC column specimens was considered as a reference specimen and identified as Specimen C. The other specimen was strengthened with RPC, then wrapped with CFRP and identified as Specimen CJF. In Algburi et al. [23], two square RC column specimens were cast with NSC. One of these two square RC column specimens was considered as a reference specimen and identified as Specimen S. The other specimen was circularized with RPC, then wrapped with CFRP and identified as Specimen SJF.

The RC column specimens were tested using a Denison compression testing machine with a capacity of 5000 kN. The data were acquired by a Data Acquisition System. The axial strain was captured by two strain gauges. The strain gauges were attached at the mid-height of two opposite longitudinal steel bars in the base circular and square RC column specimens. All the column specimens were tested under concentric axial load.

### *3.2. Experimental axial load-axial strain responses of the specimens*

The experimental axial load-axial strain responses of Specimens C and CJF are shown in Fig. 3. The service axial load of Specimen C was calculated from the transformed-section analysis using the service stress limits in ACI 440.2R-17 [27]. The service axial load of Specimen C was found to be 421 kN. Specimen C achieved an ultimate axial load of 615 kN. The ductility of Specimen C was calculated as 3.9. The final failure of Specimen C occurred by the crushing of the concrete and buckling of the longitudinal steel bars.

In general, the axial load-axial strain response of Specimen CJF included three ascending branches up to the ultimate axial load. Specimen CJF showed a quasi-linear initial axial load-axial strain response up to the axial strain of about 0.002. This was followed by an ascending branch with slope less than the slope of the initial branch. The second ascending branch of the axial load-axial strain response was associated with the confinement effect of FRP wrapping on the NSC core. The increase in the axial load continued up to the axial load corresponding to an axial strain of about 0.003. After reaching the axial strain of 0.003, the axial load-axial strain response of Specimen CJF demonstrated a slight decrease in the axial load with increasing axial strain. The decrease in the axial load was followed by the third ascending branch of the axial load-axial strain response. The slope of the third ascending branch was less than the slope of the second ascending branch. The third ascending branch of the axial load-axial strain response of Specimen CJF was associated with the confinement effect of FRP wrapping on the RPC jacket. The increase in the axial load continued up to the ultimate axial load at an axial strain of about 0.006. The service axial load of Specimen CJF was 2.1 times the service axial load of Specimen C. The ultimate axial load of Specimen CJF was 3.4 times the ultimate axial load of Specimen C. The ductility of Specimen CJF was 1.36 times the ductility of Specimen C. After the ultimate axial load, the axial load of Specimen CJF dropped in two steps to about 50% of the ultimate axial load. Afterwards, the axial load-axial strain response of Specimen CJF exhibited softening response due to the confinement effect of the lateral steel helices of the base circular RC column specimen. The softening response dominated the behavior of Specimen CJF up to the end of the test. Failure of Specimen CJF occurred by the rupture of FRP and crushing of RPC jacket at the upper one-third segment of the specimen.

The experimental axial load-axial strain responses of Specimens S and SJF are presented in Fig. 4. The service axial load of Specimen S was 573 kN. Specimen S achieved an ultimate axial load of 798 kN and a ductility of 3.3. The final failure of Specimen S occurred by the crushing of the concrete and the fracture of the steel ties. The service axial load of Specimen SJF was 2.52 times the service axial load of Specimen S. The ultimate axial load of Specimen SJF was 4.56 times the ultimate axial load of Specimen S. The ductility of Specimen SJF was 1.6 times the ductility of Specimen S. Specimen SJF failed by the rupture of FRP and crushing of RPC jacket at the mid-height of the specimen.

## 4. Comparison between the analytical and experimental axial load-axial strain responses of the strengthened RC columns

The analytical approach presented in Section 2.2 was used to plot the analytical axial load-axial strain responses of Specimens CJF and SJF using spreadsheets.

Figure 5 compares the analytical and experimental axial load-axial strain responses for the circular RC column strengthened with RPC jacket and wrapped with FRP (Specimen CJF). The initial quasi-linear portion of the analytical axial load-axial strain response matched the initial quasi-linear portion of the experimental axial load-axial strain response. However, after the compressive strain of 0.002, the analytical axial load was lower than the experimental axial load. At the compressive strain of 0.003, the analytical axial load was 87% of the experimental axial load. After the compressive strain of 0.004, the analytical axial load-axial strain response presented in this study well matched the experimental axial load-axial strain response and was conservative in predicting the ultimate axial load. At the maximum experimental compressive strain of 0.006, the analytical axial load was 98% of the experimental axial load.

Figure 6 shows the analytical and experimental axial load-axial strain responses for the square RC column circularized with RPC jacket and wrapped with FRP (Specimen SJF). The analytical and experimental axial load-axial strain responses of Specimen SJF matched well up to the compressive strain of 0.002. At the compressive strain of 0.003, the analytical axial load was 91% of the experimental axial load. Between the compressive strain of 0.004 and the maximum experimental compressive strain, the analytical axial load became closer to the experimental axial load but remained conservative. At the maximum experimental compressive strain of 0.006, the analytical axial load was 95% of the experimental axial load. In general, the analytical axial load-axial strain responses presented in this study matched well with the experimental axial load-axial strain responses for the circular and square RC columns strengthened with RPC and wrapped with FRP.

## 5. Parametric study

In the parametric study, the influences of three factors on the service axil load, ultimate axial load and ductility of the circular and square RC columns strengthened with RPC and wrapped with FRP were investigated. The first factor is the confinement ratio. The confinement ratio in this study is the ratio of the confinement pressure to the unconfined compressive strength of the strengthened RC column. The second factor is the unconfined compressive strength of the RPC jacket. The third factor is the ratio of the RPC jacket thickness to the diameter or side length of the circular or square base RC column.

To investigate the influence of the three factors on the service axial load, ultimate axial load and ductility of the strengthened RC columns, two base RC columns with circular and square cross-sections were assumed to be the existing (base) RC columns. The circular base RC column was assumed to have a diameter of 500 mm and the square base RC column was assumed to have a side length of 500 mm. The two base circular and square RC columns were assumed to be reinforced with longitudinal steel bars having a reinforcement ratio of 0.02. The yield tensile strengths of the steel bars were assumed to be 400 MPa (assumed to be deteriorated in existing structures). The NSC of the two base circular and square RC columns was assumed to have an unconfined compressive strength of 30 MPa.

Figure 7 shows the influence of the confinement ratio of the FRP wrapping on the axial load-axial strain responses of the circular and square RC columns strengthened with RPC and wrapped with FRP. The base circular RC column was assumed to be strengthened with RPC jacket with a thickness of 50 mm ($t/d = 0.1$). The base square RC column was assumed to be strengthened with RPC jacket with a thickness at the corners of the square section of 50 mm ($t_2/b = 0.03$). The RPC jacket was assumed to have an unconfined compressive strength ($f'_{cj}$) of 100 MPa. Each circular or square RC column strengthened with RPC was assumed to be wrapped with FRP of a confinement ratio ($f_l/f'_{cav}$) = 0.08, 0.15 and 0.3. The $f'_{cav}$ is the average weighted unconfined compressive strength of the NSC and RPC in the strengthened section. This parametric study showed that the confinement ratio ($f_l/f'_{cav}$) did not have any significant influence on the service axial load of the circular or square RC column strengthened with RPC and wrapped with FRP. Figure 7 shows that an increase in the $f_l/f'_{cav}$ of the circular RC column strengthened with RPC and wrapped with FRP from 0.08 to 0.3, increased the ultimate axial load and ductility by 45% and 104%, respectively. An increase in the $f_l/f'_{cav}$ of the square RC column circularized with RPC and wrapped with FRP from 0.08 to 0.3, increased the ultimate axial load and ductility by 46% and 97%, respectively.

Figure 8 shows the influence of the unconfined compressive strength of the RPC jacket ($f'_{cj}$) on the axial load-axial strain responses of the strengthened RC columns. In Fig. 8, the base RC columns were assumed to be strengthened with RPC jackets of $f'_{cj}$ = 100MPa, 150 MPa and 200 MPa. The RPC jacket thickness for the circular base RC columns ($t$) was taken as $0.1d$ and for the square base RC columns ($t_2$) was taken as $0.03b$. The $f_l/f'_{cav}$ was taken as 0.15 for the all strengthened RC columns. Figure 8 reveals that an increase in the $f'_{cj}$ of the circular RC column strengthened with RPC and wrapped with FRP from 100 MPa to 200 MPa, increased the service axial load and ultimate axial load by 16% and 45%, respectively, and decreased the ductility by 2%. An increase in the $f'_{cj}$ of the square RC column circularized with RPC and wrapped with FRP from 100 MPa to 200 MPa, increased the service axial load, ultimate axial load and ductility by 19%, 57% and 5%, respectively.

Figure 9 shows the influence of the $t/d$ ratio and $t_2/b$ ratio on the axial load-axial strain responses of the strengthened RC columns. In Fig. 9, the base circular RC column was assumed to be strengthened with RPC jacket of $t$ = $0.05d$, $0.1d$, $0.125d$ and $0.167d$. The base square RC column was assumed to be strengthened with RPC jacket of $t_2$ = $0.03b$, $0.05b$, $0.1b$ and $0.125b$. The $f'_{cj}$ was taken as 100 MPa and the $f_l/f'_{cav}$ was taken as 0.15 for all the strengthened RC columns. Figure 9 shows that an increase in the $t/d$ ratio of the circular RC column strengthened with RPC and wrapped with FRP from 0.05 MPa to 0.167 MPa, increased the service axial load, ultimate axial load and ductility by 64%, 96% and 30%, respectively. An increase in the $t_2/b$ ratio of the square RC column circularized with RPC and wrapped with FRP from 0.03 MPa to 0.125 MPa, increased the service axial load, ultimate axial load and ductility by 32%, 44% and 13%, respectively.

To achieve a significant enhancement in the axial load-axial strain response for the deficient circular or square RC column, the ratio of the RPC jacket thickness to the diameter or side length of the base RC column is recommended to be 0.1 or 0.05, respectively.

## 6. Conclusions

This study presented an analytical approach to predict the axial load-axial strain responses for circular and square RC columns strengthened with RPC and wrapped with FRP. The analytical axial load-axial strain responses were compared with experimental axial load-axial strain responses. The study also presented a parametric study to investigate the most influencing factors that affect the axial load-axial strain responses of the strengthened RC columns. Based on the results of this study, the following conclusions can be drawn:

1. The developed analytical approach takes into account the contributions of the confined NSC core, the confined RPC jacket and the steel reinforcement bars up to the ultimate axial load.
2. The analytical axial load-axial strain responses presented in this study were conservative and matched well the experimental axial load-axial strain responses.
3. Increasing the ratio of the RPC jacket thickness to the diameter or side length of the base RC column had a considerable positive influence on the service and ultimate axial loads as well as ductility of the strengthened RC column. The ratio of the RPC jacket thickness to the diameter or side length of the base RC column was found to be the most significant factor on the service axial load of the strengthened RC column. The ratio of the RPC jacket thickness to

the diameter or side length of the base RC column is recommended to be 0.1 or 0.05, respectively.

## Acknowledgements

The authors would like to acknowledge the University of Wollongong, Australia for the financial support of this study. The first author also would like to acknowledge the Iraqi Government and the Higher Committee for Education Development in Iraq for their full financial support to his PhD study. Special thanks to all technical staff in the Structural Engineering laboratory at the University of Wollongong, Australia for their technical support in the experimental program of this study.

## References

[1] E. Julio, F. Branco, V. Silva, Structural rehabilitation of columns with reinforced concrete jacketing, Progress in Structural Engineering and Materials 5(1) (2003) 29-37.

[2] E. Julio, F.A. Branco, V. Silva, Reinforced concrete jacketing-interface influence on monotonic loading response, ACI Structural Journal 102(2) (2005) 252-257.

[3] V. Marlapalle, P. Salunke, N. Gore, Analysis & design of RCC jacketing for buildings, International Journal of Recent Technology and Engineering 3 (2014) 62-63.

[4] A. Teran, J. Ruiz, Reinforced concrete jacketing of existing structures, Earthquake Engineering, 10th World Conference, Balkema, Rotterdam, 1992. p. 5107-5113.

[5] G. Minafo, M. Papia, Concrete softening effects on the axial capacity of RC jacketed circular columns, Engineering Structures 128 (2016) 215-224.

[6] A.R. Takeuti, J.B. de Hanai, A. Mirmiran, Preloaded RC columns strengthened with high-strength concrete jackets under uniaxial compression, Materials and structures 41(7) (2008) 1251-1262.

[7] G. Campione, M. Fossetti, C. Giacchino, G. Minafo, RC columns externally strengthened with RC jackets, Materials and Structures 47(10) (2014) 1715-1728.

[8] Y.-F. Wu, T. Liu, D. Oehlers, Fundamental principles that govern retrofitting of reinforced concrete columns by steel and FRP jacketing, Advances in Structural Engineering 9(4) (2006) 507-533.

[9] V.M. Karbhari, Y. Gao, Composite jacketed concrete under uniaxial compression-verification of simple design equations, Journal of materials in civil engineering 9(4) (1997) 185-193.

[10] V. Marlapalle, P. Salunke, N. Gore, Analysis & design of FRP Jacketing for Buildings, International Journal of Recent Technology and Engineering 2(9) (2014) 29-31.

[11] M.N.S. Hadi, J. Li, External reinforcement of high strength concrete columns, Composite Structures 65(3) (2004) 279-287.

[12] M.N.S. Hadi, Behaviour of eccentric loading of FRP confined fibre steel reinforced concrete columns, Construction and Building Materials 23(2) (2009) 1102-1108.

[13] M.N.S. Hadi, T.M. Pham, X. Lei, New method of strengthening reinforced concrete square columns by circularizing and wrapping with fibre-reinforced polymer or steel straps, Journal of Composites for Construction 17(2) (2013) 229-238.

[14] A.D. Mai, M.N Sheikh, M.N.S Hadi, Investigation on the behaviour of partial wrapping in comparison with full wrapping of square RC columns under different loading conditions, Construction and Building Materials 168 (2018) 153-168.

[15] L.C. Bank, Composites for construction: Structural design with FRP materials, John Wiley & Sons, 2006.

[16] L. Lam, J. Teng, Design-oriented stress-strain model for FRP-confined concrete in rectangular columns, Journal of Reinforced Plastics and Composites 22(13) (2003) 1149-1186.

[17] T.M. Pham, L.V. Doan, M.N.S. Hadi, Strengthening square reinforced concrete columns by circularisation and FRP confinement. Construction and Building Materials 49 (2013) 490-499.

[18] P. Richard, M. Cheyrezy, Composition of reactive powder concretes, Cement and concrete research 25(7) (1995) 1501-1511.

[19] A.R. Malik, S.J. Foster, Carbon fibre-reinforced polymer confined reactive powder concrete columns-experimental investigation, ACI Structural Journal 107(03) (2010) 263-271.

[20] M.-G. Lee, Y.-C. Wang, C.-T. Chiu, A preliminary study of reactive powder concrete as a new repair material, Construction and Building Materials 21(1) (2007) 182-189.

[21] T. Chang, B. Chen, J. Wang, C. Wu, Performance of Reactive Powder Concrete (RPC) with different curing conditions and its retrofitting effects on concrete member, In: Alexander et al (Eds.), Concrete Repair, Rehabilitation and Retrofitting II, Taylor & Francis Group, London, UK, 2009, pp. 1203-1208.

[22] M.N.S. Hadi, A.H.M. Algburi, M.N. Sheikh, T.C. Allister, Axial and Flexural Behaviour of Circular Reinforced Concrete Columns Strengthened with Reactive Powder Concrete Jacket and Fibre Reinforced Polymer Wrapping, Construction and Building Materials 172 (2018) 117-127.

[23] A.H.M. Algburi, M.N. Sheikh, M.N.S. Hadi, New Technique for Strengthening Square Reinforced Concrete Columns by the Circularization with Reactive Powder Concrete and

Wrapping with Fiber Reinforced Polymer, Structure and Infrastructure Engineering, Manuscript ID: NSIE-2018-0471.R1, accepted on 19 Faberuary 2019.

[24] M. Samaan, A. Mirmiran, M. Shahawy, Model of concrete confined by fiber composites, Journal of structural engineering 124 (1998) 1025-1031.

[25] L. Lam, J. Teng, Design-oriented stress–strain model for FRP-confined concrete, Construction and building materials 17 (2003) 471-489.

[26] ACI 440.2R-08, Guide for the design and construction of externally bonded FRP systems for strengthening concrete structures, American Concrete Institute, United States, 2008.

[27] ACI 440.2R-17, Guide for the design and construction of externally bonded FRP systems for strengthening concrete structures, American Concrete Institute, United States, 2017.

[28] Q. Xiao, J. Teng, T. Yu, Behavior and modeling of confined high-strength concrete, Journal of Composites for Construction 14(3) (2010) 249-259.

[29] S. Ahmad, A. Zubair, M. Maslehuddin, Effect of key mixture parameters on flow and mechanical properties of reactive powder concrete, Construction and Building Materials 99 (2015) 73-81.

[30] D.S. de Oliveira, V. Raiz, R. Carrazedo, Experimental Study on Normal-Strength, High-Strength and Ultrahigh-Strength Concrete Confined by Carbon and Glass FRP Laminates, Journal of Composites for Construction 23(1) (2018) 04018072.

[31] S. Watson, F. Zahn, R. Park, Confining reinforcement for concrete columns, Journal of Structural Engineering 120(6) (1994) 1798-1824.

## List of Figures

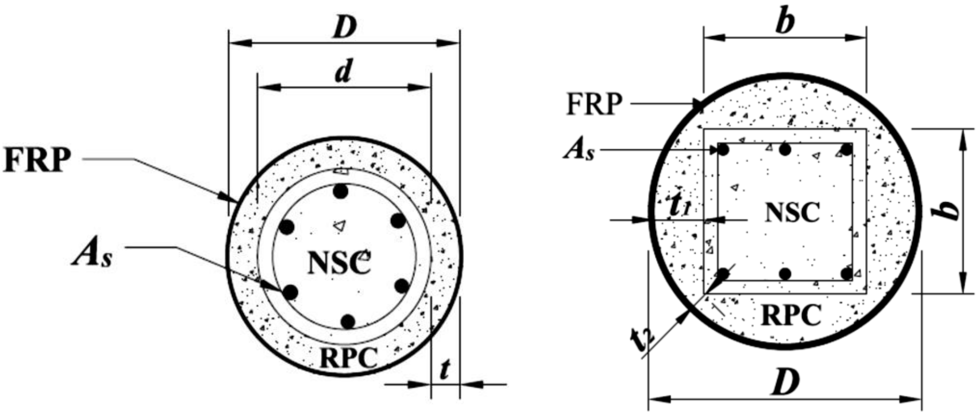


(a) (b)

Fig. 1. Cross-sections of strengthened RC columns: (a) circular RC column strengthened with RPC and wrapped with FRP and (b) square RC column circularized with RPC jacket and wrapped with FRP

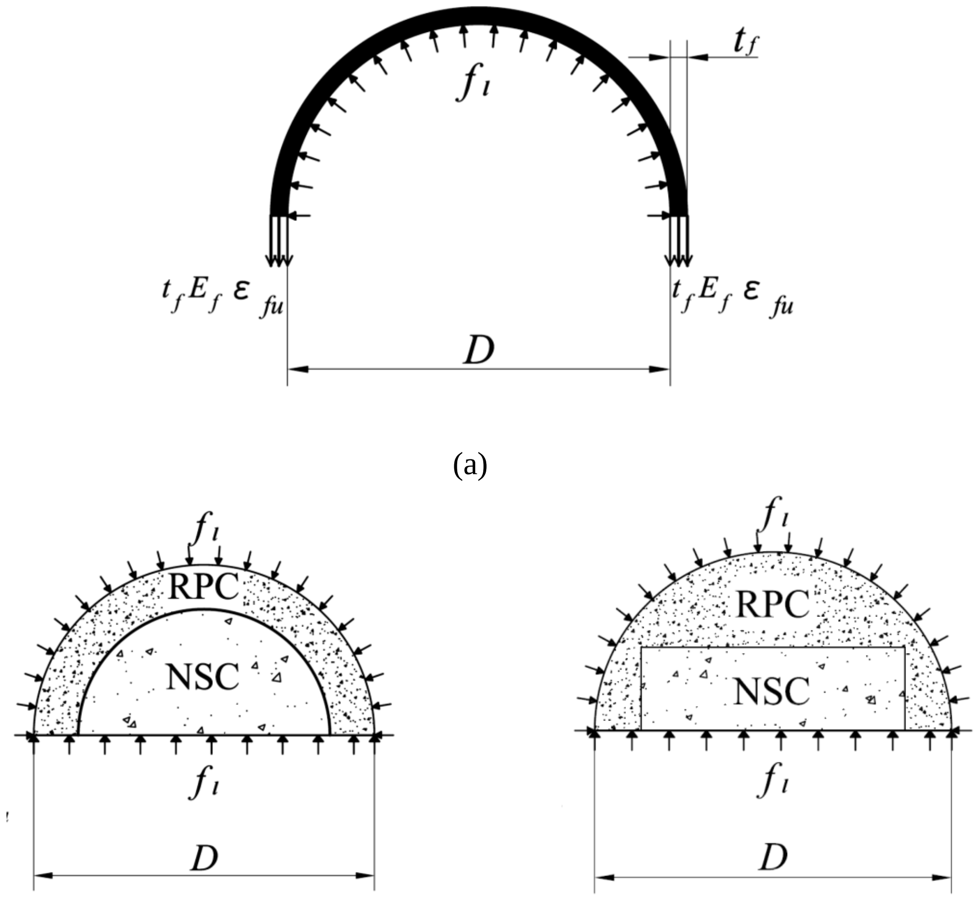


(a) (b) (c)

Fig. 2. Confinement of FRP on the NSC and RPC in the strengthened sections: (a) the FRP jacket, (b) circular column strengthened with RPC and wrapped with FRP and (c) square column circularized with RPC jacket and wrapped with FRP

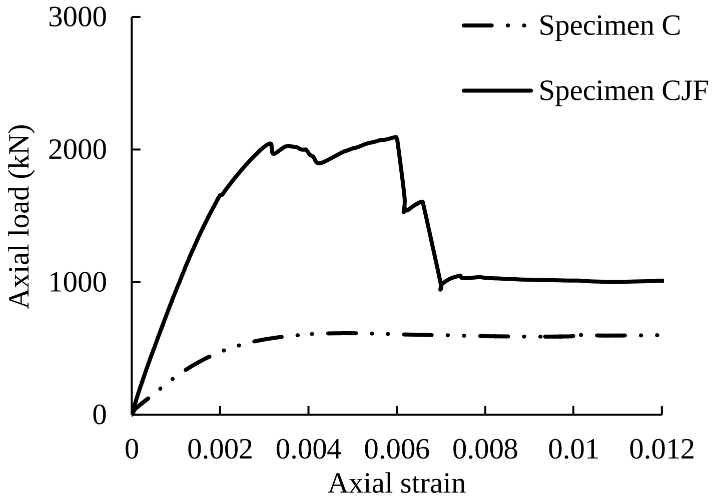


Fig. 3. Experimental axial load-axial strain responses of Specimens C and CJF

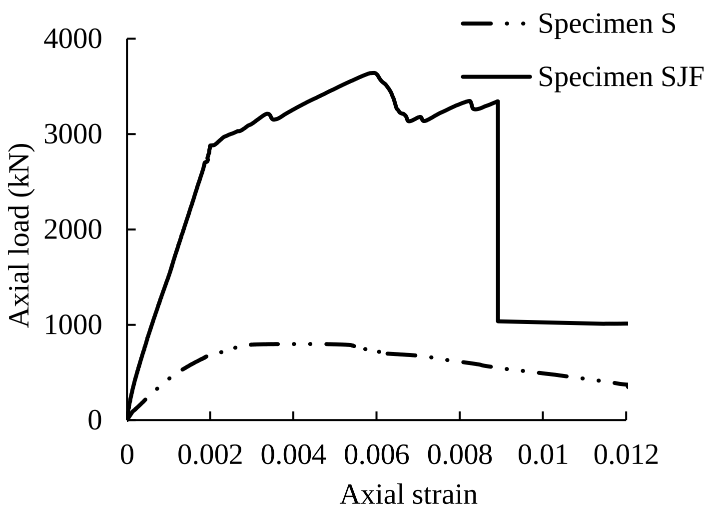


Fig. 4. Experimental axial load-axial strain responses of Specimens S and SJF

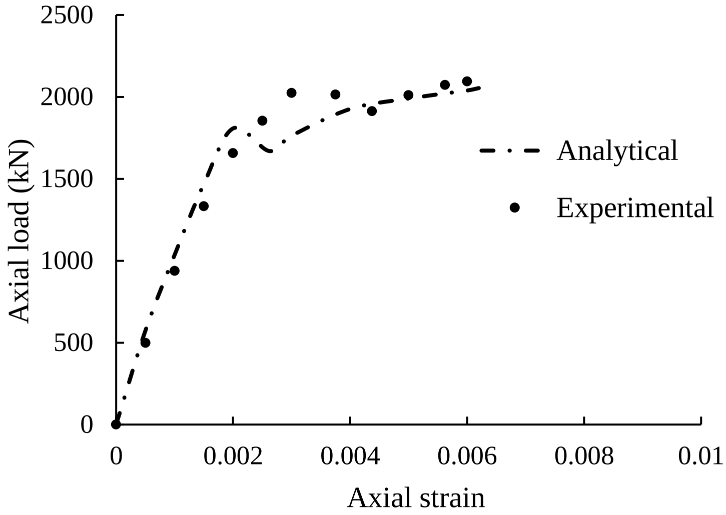


Fig. 5. Analytical and experimental axial load-axial strain responses of circular RC column strengthened with RPC and wrapped with FRP

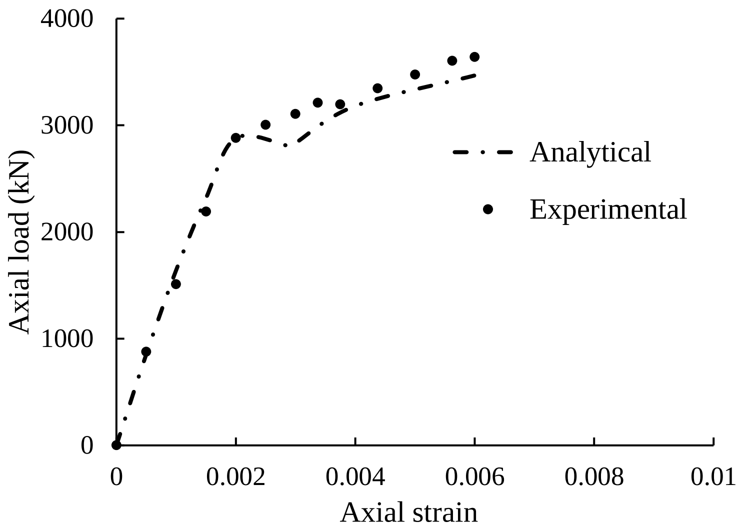


Fig. 6. Analytical and experimental axial load-axial strain responses of square RC column circularized with RPC jacket and wrapped with FRP

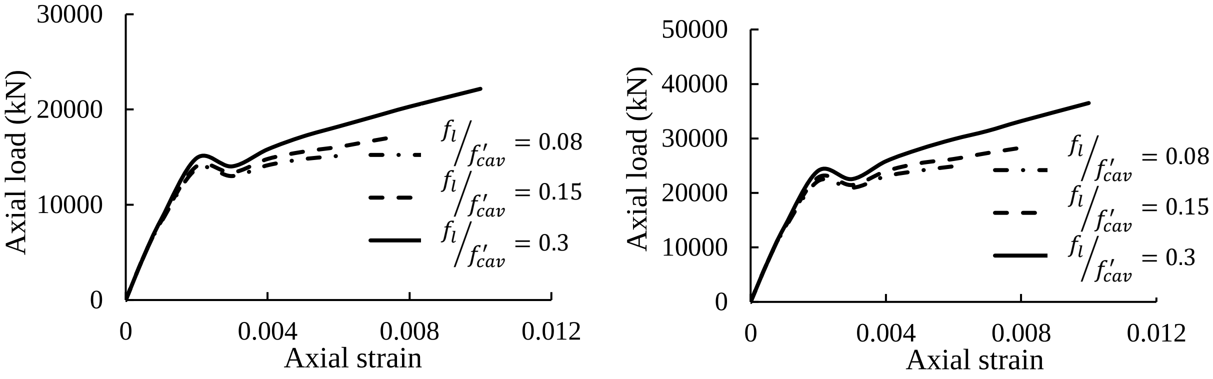


(a) (b)

Fig. 7. Influence of $f_l/f'_{cav}$ on the axial load-axial strain responses of the strengthened RC columns: (a) circular RC column strengthened with RPC and wrapped with FRP and (b) square RC column circularized with RPC jacket and wrapped with FRP

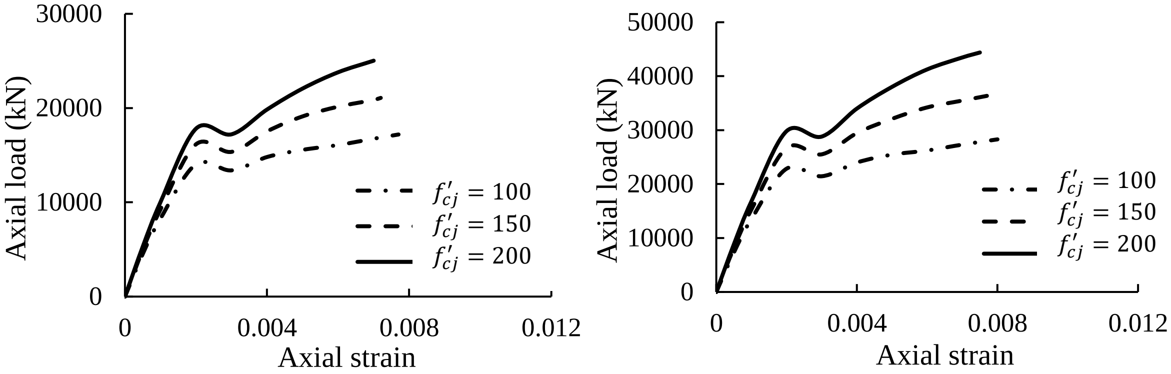


(a) (b)

Fig. 8. Influence of $f'_{cj}$ on the axial load-axial strain responses of the strengthened RC columns: (a) circular RC column strengthened with RPC and wrapped with FRP and (b) square RC column circularized with RPC jacket and wrapped with FRP

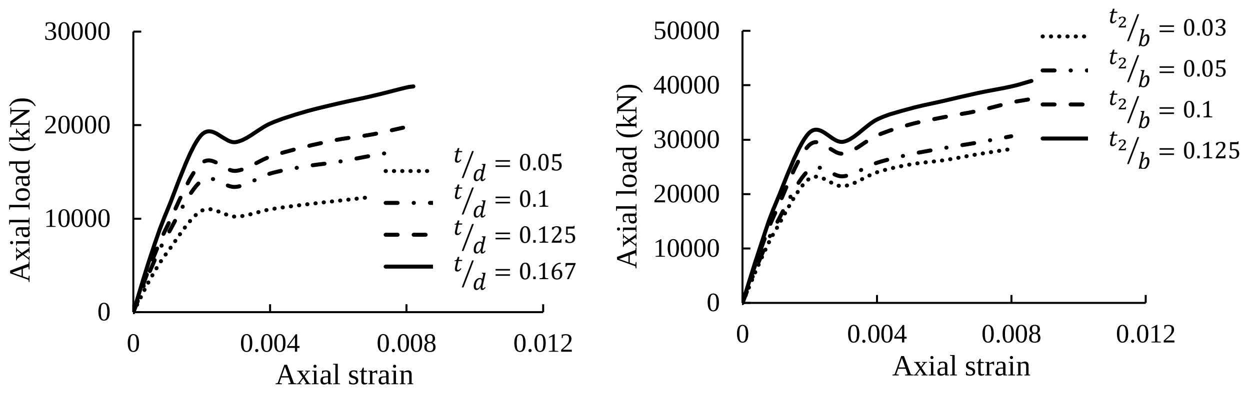


(a) (b)

Fig. 9. Influence of $t/d$ ratio and $t_2/b$ ratio on the axial load-axial strain responses of the strengthened RC columns: (a) circular RC column strengthened with RPC and wrapped with FRP and (b) square RC column circularized with RPC jacket and wrapped with FRP